

Doppler-stabilized fiber link with 6 dB noise improvement below the classical limit

Original

Doppler-stabilized fiber link with 6 dB noise improvement below the classical limit / C. E., Calosso; E. K., Bertacco; D., Calonico; C., Clivati; Costanzo, Giovanni Antonio; M., Frittelli; F., Levi; S., Micalizio; A., Mura; A., Godone. - In: OPTICS LETTERS. - ISSN 0146-9592. - STAMPA. - 40:2(2015), pp. 131-134. [10.1364/OL.40.000131]

Availability:

This version is available at: 11583/2584403 since:

Publisher:

OSA

Published

DOI:10.1364/OL.40.000131

Terms of use:

This article is made available under terms and conditions as specified in the corresponding bibliographic description in the repository

Publisher copyright

(Article begins on next page)

Doppler-stabilized fiber link with 6 dB noise improvement below the classical limit

C. E. Calosso¹, E. Bertacco¹, D. Calonico¹, C. Clivati^{*1},
G. A. Costanzo^{1,2}, M. Frittelli^{1,2}, F. Levi¹, S. Micalizio¹, A. Mura¹, A. Godone¹

¹*Istituto Nazionale di Ricerca Metrologica INRIM, strada delle Cacce 91, 10135, Torino, Italy*

²*Politecnico di Torino, Corso Duca degli Abruzzi 24, 10129, Torino, Italy*

**Corresponding author: c.clivati@inrim.it*

It is known that temperature variations and acoustic noise affect ultrastable frequency dissemination along optical fiber. Active stabilization techniques are adopted to compensate for the fiber-induced phase noise. However, despite this compensation, the ultimate link performances are limited by the delay-unsuppressed noise that is related to the propagation delay of the light in the fiber. We demonstrate a post-processing approach which enables us to overcome this limit. We implement a subtraction algorithm between the optical signal delivered at the remote link end and the round-trip signal. In this way, a 6 dB improvement beyond the delay-unsuppressed noise is obtained. We confirm the prediction with experimental data obtained on a 47 km metropolitan fiber link and propose how to extend this method for frequency dissemination.

In the last decade, optical fiber links for frequency dissemination have become a key tool in frequency metrology. The coherent transfer of optical [1–5] and radio-frequency signals [6–9] through optical fibers encompasses the present satellite techniques in terms of resolution, enabling a number of significant applications, such as the remote comparison of atomic clocks at the 10^{-18} uncertainty level [10–12] and the investigation of new frontiers in fundamental physics, in geodesy [13] and in radioastronomy [14].

Coherent frequency links through optical fiber are based on the transfer of an ultrastable laser frequency signal along a standard telecom fiber. It is well known that length variations due to temperature and mechanical stresses affect the fiber, resulting in a severe deterioration of the delivered signal phase stability. To overcome this difficulty, it is a common practice to adopt a Doppler noise cancellation scheme in which a double pass of the light in the fiber in opposite directions is exploited [15]. Basically, from the link remote end, a part of the radiation is reflected back to the local laboratory and here phase-compared to the original signal. Their beat note allows the detection of the fiber phase noise, which is actively cancelled through a phase-locked loop. Hence, at the remote end, the beat note between the delivered laser and the local frequency reference is in principle not affected by the fiber phase noise [3]. Actually, the round-trip delay imposes an ultimate limit to the link noise suppression. In fact, the phase noise detection and cancellation is accomplished on the round-trip signal, whereas the delivered signal travels the fiber in a single pass and suffers from a residual noise due to the fiber delay. Even for a perfect Doppler cancellation at the local laboratory, the noise reduction factor on the delivered signal is $\frac{1}{3}(2\pi f\tau)^2$ for Fourier frequencies $f \ll \frac{1}{\tau}$, where τ is the one-way propagation time. [3].

The main applications of optical links are two: either the signal is directly used as an optical frequency reference or, in most of the cases, it is post-processed to perform, for instance, clocks comparisons and spectroscopy.

In this letter, we describe a novel technique that implements the real-time frequency dissemination at the level of existing Doppler-stabilized links and enables the post-processed dissemination at an improved level of stability. We also report on the experimental results we obtained on a 47 km-long optical link deployed in the metropolitan area and used for data transmission as well.

The scheme we propose is still based on the typical architecture of Doppler-stabilized optical links. However, unlike the common procedure, we only measure the phases of the local and remote beat notes, without implementing any active control loop. A convenient data processing allows to minimize the delay-unsuppressed noise, leading to a 6 dB improvement of this limit.

As in the Doppler cancellation technique, we intend to compensate the phase of the optical signal delivered at the remote link end, $\varphi_r(t)$, by detecting the phase of the beatnote between the original and the round-trip radiation, $\varphi_{rt}(t)$. As a first step, we evaluate the relation between the fiber phase noise and the phase noise of the signal transmitted at the remote link end in terms of their time evolution, following the approach described in [3]. If $\delta\varphi(z, t)dz$ is the phase noise on the fiber at time t and position z , $\varphi_r(t)$ can be written as:

$$\varphi_r(t) = \int_0^L \delta\varphi\left(z, t - \tau + \frac{z}{c_n}\right) dz \quad (1)$$

where L is the link length, c_n is the speed of light in the fiber and $\tau = L/c_n$ is the link delay. The phase noise $\varphi_{rt}(t)$ accumulated by the light on the round-trip is:

$$\begin{aligned} \varphi_{rt}(t) &= \int_0^L \left[\delta\varphi\left(z, t - 2\tau + \frac{z}{c_n}\right) + \delta\varphi\left(z, t - \frac{z}{c_n}\right) \right] dz \\ &\approx \int_0^L 2\delta\varphi(z, t - \tau) dz \end{aligned} \quad (2)$$

In Eq. (2), the approximation assumes a linear trend of the fiber perturbation at position z between the forward

and the backward paths. This is justified for perturbations which act on timescales much longer than τ , that is the case of interest in most applications. Within this approximation, the phase noise in $z = L$ is compensated by subtracting half of the round-trip signal phase from the forward signal phase:

$$\varphi_{r,\text{comp}}(t) = \varphi_r(t) - \frac{1}{2}\varphi_{rt}(t) \quad (3)$$

where the factor $1/2$ takes into account that the noise estimation is performed on a double pass in the fiber. From Eqs. (1-3), $\varphi_{r,\text{comp}}(t)$ can be calculated as:

$$\begin{aligned} \varphi_{r,\text{comp}}(t) &\approx \int_0^L \left[\delta\varphi\left(z, t - \tau + \frac{z}{c_n}\right) - \delta\varphi\left(z, t - \tau\right) \right] dz \\ &\approx \int_0^L \frac{z}{c_n} \frac{\partial}{\partial t} \delta\varphi(z, t) dz = \int_0^L h(z, t) * \delta\varphi(z, t) dz \end{aligned} \quad (4)$$

In the second line of Eq. (4), the difference between $\delta\varphi(z, t - \tau + z/c_n)$ and $\delta\varphi(z, t - \tau)$ has been rewritten in terms of their time derivative. Again, this is justified for perturbations which act on timescales much longer than τ . In the last step, we introduced $h(z, t) = \frac{z}{c_n} \dot{\delta}(t)$, with $\dot{\delta}(t)$ the time derivative of the Dirac delta generalized function. $h(z, t)$ is the impulse response that, for each z , processes the local phase perturbation. Considering the contribution of each fiber segment with length dz , we can apply the fundamental theorem of spectral analysis [16] that expresses the power spectrum of the output of a linear and time-invariant system in terms of the input power spectrum. In our case,

$$S_{r,\text{comp}}(z, f) = |H(z, f)|^2 S_{\delta\varphi}(z, f) \quad (5)$$

where $S_{r,\text{comp}}(z, f)$ and $S_{\delta\varphi}(z, f)$ are the noise spectral density contributions of a section dz of fiber at position z for the compensated and free fiber respectively. $|H(z, f)|^2 = (2\pi f z/c_n)^2$ is the square modulus of the $h(z, t)$ Fourier transform, i.e. the transfer function. If the noise is uncorrelated along the fiber, the noise contributions coming from different z positions are independent and sum up, so that we can write:

$$S_{r,\text{comp}}(f) = \int_0^L |H(z, f)|^2 S_{\delta\varphi}(z, f) dz. \quad (6)$$

Assuming, in addition, that the fiber noise is uniformly distributed along the link, i.e. $S_{\delta\varphi}(z, f) = S_r(f)/L$, an integration leads to:

$$S_{r,\text{comp}}(f) = \frac{1}{3}(2\pi f \tau)^2 S_r(f) \quad (7)$$

where $S_r(f)$ is the phase noise power spectrum of the fiber. Although this result has been obtained in a passive approach, where the round-trip fiber noise is measured and used to correct the forward signal, the same

limitation is found for actively compensated links [3]. We point out that we do not assume that the power spectrum of $\varphi(t)$ is the square modulus of its Fourier transforms. In our approach, Eq. (7) is deduced from the definition of power spectral density in terms of the Fourier transform of its autocorrelation, i.e. the formal definition in the case of random processes [16, 17].

To improve the limit posed by Eq. (7), we reconsider Eq. (3) supposing that the subtraction can be performed between arbitrarily time-delayed samples, with delay α :

$$\tilde{\varphi}_{r,\text{comp}}(t) = \varphi_r(t) - \frac{1}{2}\varphi_{rt}(t + \alpha) \quad (8)$$

where $\tilde{\varphi}_{r,\text{comp}}$ is the corresponding compensated phase. With the same assumptions adopted previously, i.e. noise uncorrelated and uniformly distributed along the link, Eqs. (6) and (7) are modified into:

$$\begin{aligned} \tilde{S}_{r,\text{comp}}(f) &= \int_0^L |\tilde{H}(z, f)|^2 S_{\delta\varphi}(z, f) dz \\ &= \frac{1}{3}(2\pi f)^2 (\tau^2 - 3\alpha\tau + 3\alpha^2) S_r(f) \end{aligned} \quad (9)$$

where $|\tilde{H}(z, f)|^2 = (2\pi f)^2 (z/c_n - \alpha)^2$. The noise conversion is minimized for $\alpha = \tau/2$ leading to:

$$\tilde{S}_{r,\text{comp}}(f) = \frac{1}{12}(2\pi f \tau)^2 S_r(f) \quad (10)$$

The remarkable result expressed by Eq. (10) is that performing the subtraction of time-shifted phase data, the limit shown in Eq. (7) is overcome by 6 dB. More specifically, the noise compensation is optimized if the round-trip signal is shifted by $\tau/2$. This of course can be done only by post-processing the phases φ_r and φ_{rt} acquired at both sides of the fiber. The synchronization is not a stringent requirement: in a real case, timing at the level of $\tau/10$ is feasible and is widely enough for most applications [18]. This has been demonstrated in [19] and the same approach can be followed in this context.

To verify the theoretical prediction of Eq. (10), we implement the setup shown in Fig. 1. A narrow-linewidth laser is generated by frequency-locking a fiber laser to a high-finesse Fabry-Pérot cavity at the 10^{-14} stability level at 1 s [20]. The laser is split into two parts: a small fraction of the optical power is used as a local oscillator, the other part travels the optical link. This is based on a 47 km-long optical fiber buried in the metropolitan area of Turin (Italy), with both ends in our laboratory. Accordingly, $\tau = 235 \mu\text{s}$ for this loop. The fiber is implemented on a Dense Wavelength Division Multiplexed (DWDM) architecture where the channel 44 of the International Telecommunication Union grid is dedicated to this experiment, whereas channels 21 and 22 are occupied by the Internet traffic. More details about this fiber loop can be found in [21]. At the remote link end, the radiation is frequency shifted by 40 MHz by the acousto-optic modulator AOM to distinguish the round-trip signal from the stray reflections along the fiber. A fraction

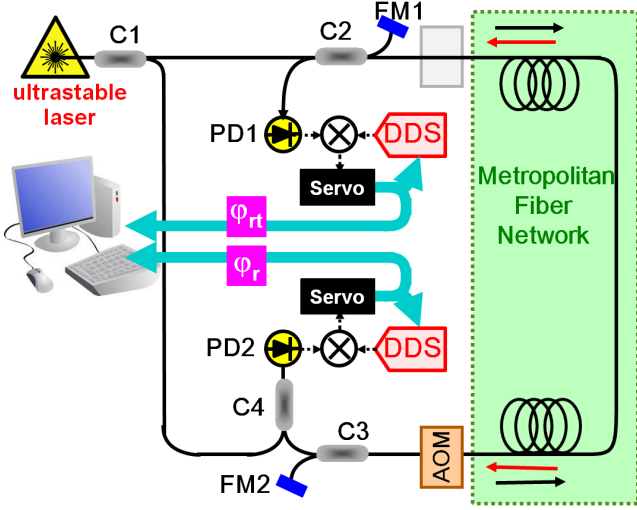


FIG. 1. The experimental setup. The ultrastable laser is split into two beams. A part is used as a local oscillator; the other part travels the link and, at the remote end, is frequency shifted by the acousto-optic modulator AOM, extracted and compared to the local oscillator on photodiode PD2. A part of the light is reflected by the Faraday mirror FM2 and travels the link in the backward direction; the round-trip light is compared to the local oscillator on photodiode PD1; C1-C4 represent optical couplers. The beat notes on PD1 and PD2 are tracked by two Direct Digital Synthesizers (DDSs); the phase corrections φ_{rt} and φ_r are also sent to a PC for measurement. The grey empty box indicates the position where AOM' would be placed for the active link stabilization.

of the delivered radiation is extracted and compared to the original one on photodiode PD2; this enables to directly measure the link performances, rejecting the laser noise contribution. The other part is reflected by a Faraday mirror to the local laboratory and here beaten with the original laser on photodiode PD1, to detect the fiber noise. In a real case where the laser is not in common mode, PD2 directly measures the phase difference between the local and the received optical signal.

The phases of the beat notes on PD1 and PD2 represent the phase noises of the round-trip and of the forward signal respectively. They are measured with a digital and synchronous electronic system in which two Direct Digital Synthesizers (DDSs) [19, 22] track the beat notes through a phase-locked loop (PLL). In particular, a double balanced mixer is used as phase discriminator; φ_r and φ_{rt} are recorded with a sampling rate of 4 kHz and a measurement bandwidth of 2 kHz, then a Field Programmable Gate Array (FPGA) implements the servos and drives the phase of the DDSs. Within the PLL bandwidth, the data sent to the DDSs coincide with the phases of the beat notes numerically expressed, which can thus be retrieved. Then, we apply the algorithms exposed in Eqs. (3) and (8) by post-processing.

Figure 2 shows the power spectral densities of the signals of interest: the free-running fiber noise $S_r(f)$ (blue

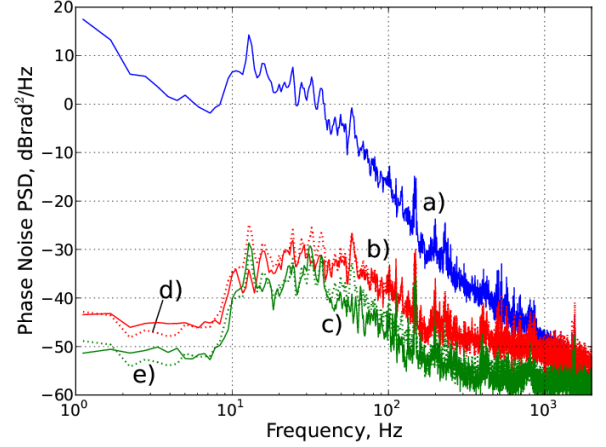


FIG. 2. The phase noise power spectra measured at the remote end. Blue line (a): the free running fiber, red line (b): the compensated phase noise with synchronous subtraction, green line (c): the compensated phase noise with a $\tau/2$ shift between samples. Dotted lines (d) and (e) show the predictions in the two cases, according to Eq. (3) and Eq. (8).

line, a) and the compensated signals, both when the samples are subtracted synchronously (red line, b) and when a $\tau/2$ time shift is applied (green line, c). Dotted lines (d) and (e) represent the expected limitations in the two cases. It can be seen that the measurements are in good agreement with the predictions and that the noise suppression is improved by 6 dB at frequencies $f \ll \frac{1}{\tau}$ for time-shifted samples. The link noise contribution to the distant clocks comparison can then be reduced by a factor of 2 in terms of frequency stability if a proper subtraction algorithm is implemented; this increases the resolution or, which is the same, allows the reduction of the measurement time needed for the comparison.

It is interesting to note that this scheme can be applied to existing Doppler-stabilized links as well. To figure out, in principle, how this can be done, we consider again the setup of Fig. 1, where another acousto-optic modulator AOM' is inserted between the coupler C2 and the fiber as an actuator for the active link stabilization. Considering the effect of its phase modulation φ_c on the round-trip and on the forward signals, we obtain:

$$\begin{aligned}\varphi_r(t) &= \varphi_r^{cl}(t) - \varphi_c(t - \tau) \\ \varphi_{rt}(t) &= \varphi_{rt}^{cl}(t) - \varphi_c(t - 2\tau) - \varphi_c(t)\end{aligned}\quad (11)$$

The superscript “cl” identifies the signals in the closed loop approach. According to Eq. (11), we rewrite Eq. (8) as a function of the signals in closed loop:

$$\begin{aligned}\tilde{\varphi}_{r,comp}(t) &= \varphi_r(t) - \frac{1}{2}\varphi_{rt}\left(t + \frac{\tau}{2}\right) \\ &= \varphi_r^{cl}(t) - r(t)\end{aligned}\quad (12)$$

where we define $r(t)$ as follows:

$$r(t) = \varphi_c(t - \tau) + \frac{\varphi_{\text{rt}}^{\text{cl}}(t + \frac{\tau}{2}) - \varphi_c(t - \frac{3}{2}\tau) - \varphi_c(t + \frac{\tau}{2})}{2} \quad (13)$$

$r(t)$ represents a realignment term, which can be measured in the local laboratory by synchronously acquiring the phase-correction $\varphi_c(t)$ imposed to AOM' and the PD1 beat note phase when the controller is active. This term can then be applied to the phase measurement at the remote end, to improve the comparison during post-processing. Thus, the frequency dissemination is performed at the classical limit; in addition, the phase-measurement can be further processed to obtain the 6 dB improvement.

In conclusion, we demonstrate from a theoretical and an experimental point of view that the classical limit in the phase-stabilization of coherent optical links can be overcome by time-shifting the phase correction applied to the forward signal. Without a loss of generality, this improvement is demonstrated in a passive approach, where there is no active cancellation of the fiber noise. Furthermore, we suggest how to improve the apparatus

to perform two tasks at the same time: the delivery of an ultrastable frequency signal and the off-line processing to increase the resolution in a frequency comparison. The digital implementation ensures a precise timing of the measurements, which is essential for the synchronous acquisition, is reliable and easily adapted to perform different tasks. This is particularly interesting for the next generation of atomic clocks, which are expected to achieve the 10^{-18} level of relative frequency stability in 100s of averaging time [10–12]. In addition, it may benefit other applications, such as the long-haul fiber frequency dissemination, paving the way for new measurements in atomic and fundamental physics.

We thank Luca Lorini for useful discussion and careful reading of the manuscript and Consortium GARR for technical help with the fibers. This work was partly funded by Compagnia di San Paolo, by MIUR under Progetto Premiale 2012, and by the EMRP programs SIB02-NEAT-FT and IND55-MClocks. The EMRP is jointly funded by the EMRP participating countries within EURAMET and the European Union.

-
- [1] K. Predehl, G. Grosche, S. M. F. Raupach, S. Droste, O. Terra, J. Alnis, Th. Legero, T. W. Hänsch, Th. Udem, R. Holzwarth, H. Schnatz, *Science* **336**, 441 (2012).
 - [2] O. Lopez, A. Haboucha, B. Chanteau, Ch. Chardonnet, A. Amy-Klein, G. Santarelli, *Opt. Expr.* **20**, 23518 (2012).
 - [3] W. Williams, W. C. Swann, N. R. Newbury, *J. Opt. Soc. Am. B* **25**, 1284 (2008).
 - [4] D. Calonico, E. K. Bertacco, C. E. Calosso, C. Clivati, G. A. Costanzo, M. Frittelli, A. Godone, A. Mura, N. Poli, D. V. Sutyryn, G. M. Tino, M. E. Zucco, F. Levi, *Appl. Phys. B*, in press, DOI 10.1007/s00340-014-5917-8.
 - [5] M. Fujieda, M. Kumagai, S. Nagano, A. Yamaguchi, H. Hachisu, and T. Ido, *Opt. Expr.* **19**, 16498 (2011).
 - [6] L. Śliwczynski, P. Krehlik, A. Czubla, L. Buczek, M. Lipiński, *Metrologia* **50**, 133 (2013).
 - [7] Y. He, B. J. Orr, K. G. H. Baldwin, M. J. Wouters, A. N. Luiten, G. Aben, R. B. Warrington *Opt. Expr.* **21**, 18754 (2013).
 - [8] B. Wang, C. Gao, W.L. Chen, J. Miao, X. Zhu, Y. Bai, J.W. Zhang, Y.Y. Feng, T.C. Li, L.J. Wang, *Sci. Rep.* **2**, 556 (2012).
 - [9] G. Marra, H. S. Margolis, D. J. Richardson, *Opt. Expr.* **20**, 1775 (2012).
 - [10] B. J. Bloom, T. L. Nicholson, J. R. Williams, S. L. Campbell, M. Bishof, X. Zhang, W. Zhang, S. L. Bromley, J. Ye, *Nature* **506**, 7175 (2014).
 - [11] I. Ushijima, M. Takamoto, M. Das, T. Ohkubo, H. Katori, arXiv:1405.4071 (2014).
 - [12] N. Hinkley, J. A. Sherman, N. B. Phillips, M. Schioppo, N. D. Lemke, K. Beloy, M. Pizzocaro, C. W. Oates, A. D. Ludlow, *Science* **341**, 1215-1218 (2013).
 - [13] C. W. Chou, D. B. Hume, T. Rosenband, D. J. Wineland, *Science* **329**, 1630 (2010).
 - [14] J.-F. Cliché, B. Shillue, *IEEE Control Sys. Mag.* **26**, 19 (2006).
 - [15] L.-S. Ma, P. Jungner, J. Ye, J. L. Hall, *Opt. Lett.* **19**, 1777-1779 (1994).
 - [16] A. Papoulis, "Probability, Random Variables, and Stochastic Processes," International Student Edition, McGraw Hill and Kogakusha company, Ltd. 1965, p. 347.
 - [17] Bercy, S. Guellati-Khelifa, F. Stefani, G. Santarelli, Ch. Chardonnet, P-E. Pottier, O. Lopez, A. Amy-Klein, *J. Opt. Soc. Am. B* **31**, 678-685 (2014).
 - [18] S. M. F. Raupach and G. Grosche, *IEEE Trans. on Ultrason. Ferroel. Freq. Contr.* **61**, 920-929 (2014).
 - [19] C. E. Calosso, E. Bertacco, D. Calonico, C. Clivati, G. A. Costanzo, M. Frittelli, F. Levi, A. Mura, A. Godone, *Opt. Lett.* **39**, 1177 (2014).
 - [20] C. Clivati, D. Calonico, C. E. Calosso, G. A. Costanzo, F. Levi, A. Mura, A. Godone, *IEEE Trans. Ultrason. Ferroelectr. Freq. Contr.* **58**, 2582 (2011).
 - [21] C. Clivati, D. Calonico, G. A. Costanzo, A. Mura, M. Pizzocaro, F. Levi, *Opt. Lett.* **38**, 1092-1094 (2013).
 - [22] C. E. Calosso, in *Proceedings of the Joint UFFC, EFTF and PFM Symposium (2013)*, p. 747.

1. K. Predehl, G. Grosche, S. M. F. Raupach, S. Droste, O. Terra, J. Alnis, Th. Legero, T. W. Hänsch, Th. Udem, R. Holzwarth, H. Schnatz, "A 920-Kilometer Optical Fiber Link for Frequency Metrology at the 19th decimal place," *Science* **336**, 441 (2012).
2. O. Lopez, A. Haboucha, B. Chanteau, Ch. Chardonnet, A. Amy-Klein, G. Santarelli, "Ultra-stable long distance optical frequency distribution using the Internet fiber network," *Opt. Expr.* **20**, 23518 (2012).
3. W. Williams, W. C. Swann, N. R. Newbury, "High-stability transfer of an optical frequency over long fiber optic links," *J. Opt. Soc. Am. B* **25**, 1284 (2008).
4. D. Calonico, E. K. Bertacco, C. E. Calosso, C. Clivati, G. A. Costanzo, M. Frittelli, A. Godone, A. Mura, N. Poli, D. V. Sutyryn, G. M. Tino, M. E. Zucco, F. Levi, "High accuracy coherent optical frequency transfer over a doubled 642 km fiber link," *Appl. Phys. B*, in press (2014), DOI 10.1007/s00340-014-5917-8.
5. M. Fujieda, M. Kumagai, S. Nagano, A. Yamaguchi, H. Hachisu, and T. Ido, "All optical link for direct comparison of distant optical clocks," *Opt. Expr.* **19**, 16498 (2011).
6. L. Śliwczyński, P. Krehlik, A. Czubla, L. Buczek, M. Lipiński, "Dissemination of time and RF frequency via a stabilized fibre optic link over a distance of 420 km," *Metrologia* **50**, 133 (2013).
7. Y. He, B. J. Orr, K. G. H. Baldwin, M. J. Wouters, A. N. Luiten, G. Aben, R. B. Warrington, "Stable radio-frequency transfer over optical fiber by phase-conjugate frequency mixing," *Opt. Expr.* **21**, 18754 (2013).
8. B. Wang, C. Gao, W.L. Chen, J. Miao, X. Zhu, Y. Bai, J.W. Zhang, Y.Y. Feng, T.C. Li, L.J. Wang, "Precise and continuous time and frequency synchronization at the 5×10^{-19} Accuracy Level," *Sci. Rep.* **2**, 556 (2012).
9. G. Marra, H. S. Margolis, D. J. Richardson, "High resolution microwave frequency transfer over a 86 km long optical fiber network using an optical frequency comb," *Opt. Expr.* **20**, 1775 (2012).
10. B. J. Bloom, T. L. Nicholson, J. R. Williams, S. L. Campbell, M. Bishof, X. Zhang, W. Zhang, S. L. Bromley, J. Ye, "An optical lattice clock with accuracy and stability at the 10⁻¹⁸ level," *Nature* **506**, 7175 (2014).
11. I. Ushijima, M. Takamoto, M. Das, T. Ohkubo, H. Katori "Cryogenic optical lattice clocks with a relative frequency difference of 1×10^{-18} ," arXiv:1405.4071 (2014).
12. N. Hinkley, J. A. Sherman, N. B. Phillips, M. Schioppo, N. D. Lemke, K. Beloy, M. Pizzocaro, C. W. Oates, A. D. Ludlow, "An Atomic Clock with 10^{-18} Instability," *Science* **341**, 1215-1218 (2013).
13. C. W. Chou, D. B. Hume, T. Rosenband, D. J. Wineland, "Optical clocks and relativity," *Science* **329**, 1630 (2010).
14. J.-F. Cliché, B. Shillue, "Precision timing control for radioastronomy: maintaining femtosecond synchronization in the Atacama Large Millimeter Array," *IEEE Control Sys. Mag.* **26**, 19 (2006).
15. L-S. Ma, P. Jungner, J. Ye, J. L. Hall, "Delivering the same optical frequency at two places: accurate cancellation of phase noise introduced by an optical fiber or other time-varying path," *Opt. Lett.* **19**, 1777-1779 (1994).
16. A. Papoulis, "Probability, Random Variables, and Stochastic Processes," International Student Edition, McGraw Hill and Kogakusha company, ltd. 1965, p. 347.
17. Bercy, S. Guellati-Khelifa, F. Stefani, G. Santarelli, Ch. Chardonnet, P-E. Pottie, O. Lopez, A. Amy-Klein, "In-line extraction of an ultrastable frequency signal over an optical fiber link," *J. Opt. Soc. Am. B* **31**, 678-685 (2014).
18. S. M. F. Raupach and G. Grosche "Measuring the Relative Synchronization Error of Remote Frequency Counters on the Sub-ms Level via a Phase Stabilized Fiber Link," *IEEE Trans. on Ultrason. Ferroel. Freq. Contr.* **61**, 920-929 (2014).
19. C. E. Calosso, E. Bertacco, D. Calonico, C. Clivati, G. A. Costanzo, M. Frittelli, F. Levi, A. Mura, A. Godone, "Frequency transfer via a two-way optical phase comparison on a multiplexed fiber network," *Opt. Lett.* **39**, 1177 (2014).
20. C. Clivati, D. Calonico, C. E. Calosso, G. A. Costanzo, F. Levi, A. Mura, A. Godone, "Planar-waveguide external cavity laser stabilization for an optical link with 10^{-19} frequency stability," *IEEE Trans. Ultrason. Ferroelectr. Freq. Contr.* **58**, 2582 (2011).
21. C. Clivati, D. Calonico, G. A. Costanzo, A. Mura, M. Pizzocaro, F. Levi, "Large-area fiber-optic gyroscope on a multiplexed fiber network," *Opt. Lett.* **38**, 1092-1094 (2013).
22. C. E. Calosso, "Tracking DDS in frequency metrology," in *Proceedings of the Joint UFFC, EFTF and PFM Symposium (2013)*, p. 747.